Magnetohydrodynamic Production of Relativistic Jets

David L. Meier, *et al.*

Science **291**, 84 (2001);
DOI: 10.1126/science.291.5501.84

40. J. Norris, G. Marani, J. Bonnell, *Astrophys. J.* **534**, 248 (2000).
41. E. Fenimore, E. Ramirez-Ruiz, in preparation (available at http://xxx.lanl.gov/abs/astro-ph/0004176).
42. D. Reichart *et al.*, in preparation (available at http://xxx.lanl.gov/abs/astro-ph/0004302).
43. S. Woosley, *Astrophys. J.* **405**, 273 (1993).
44. B. Paczyński, *Astrophys. J.* **494**, L45 (1998).
45. C. Fryer, S. Woosley, D. Hartmann, *Astrophys. J.* **526**, 152 (1999).
46. Hypernovae (*44*) are massive rotating stars whose core collapse is expected to lead to a BH accreting from a debris torus resulting in a GRB, as well as the ejection of a supernova remnant shell of energy above that of usual supernovae. Collapsars (*45*) are massive stars, which in the course of merging with a compact companion undergo core collapse leading to a BH, some of which result in a GRB, leaving a supernova-like remnant. Magnetars are ultrahigh magnetic field ($B \gtrsim 10^{15}$ G), fast-rotating (initially ≳millisecond period) neutron stars, essentially super-pulsars (*50, 51*) resulting in a GRB; they would be created by the collapse of a massive rotating star leaving a supernova remnant. A supranova (*62*) is a massive star whose initial core collapse would lead to a neutron star and an ejected supernova remnant; this precedes by days to weeks a second collapse of the neutron star into a BH, which leads to a GRB. NS-NS and NS-BH mergers (*12*) also lead to a BH accreting from a debris torus, which wold be expected to lead to a GRB of comparable energy to those from massive stars (*49*); supernova remnants from the formation of the initial NS or BH would have occurred and dissipated ≳10^7 to 10^8 years before the GRB. In all of these cases, strong magnetic fields and $e^{\pm}$, γ from neutrino-antineutrino annihilation are expected to drive a jet-like relativistic outflow that leads to the standard fireball shock production of GRB and afterglows (*44, 45, 48*). In the massive progenitor cases, this would occur after the jet funnels through the stellar envelope, probably leading to a highly collimated jet, whereas in the NS-NS and NS-BH mergers the lack of an envelope might lead to substantially less collimation.
47. D. Eichler, M. Livio, T. Piran, D. N. Schramm, *Nature* **340**, 126 (1989).
48. P. Mészáros, M. J. Rees, *Astrophys. J.* **482**, L29 (1997).
49. _____, R. Wijers, *New Astron.* **4**, 313 (1999).
50. V. V. Usov, *Mon. Not. R. Astron. Soc.* **267**, 1035 (1994).
51. C. Thompson, *Mon. Not. R. Astron. Soc.* **270**, 480 (1994).
52. H. C. Spruit, *Astron. Astrophys.* **341**, L1 (1999).
53. R. D. Blandford, J. P. Ostriker, P. Mészáros, in preparation.
54. High Energy Transient Explorer (http://space.mit.edu/HETE).
55. Swift (http://swift.gsfc.nasa.gov).
56. T. Galama, R. Wijers, in preparation (available at http://xxx.lanl.gov/abs/astro-ph/0009367).
57. P. Mészáros, M. J. Rees, *Mon. Not. R. Astron. Soc.* **299**, L10 (1998).
58. C. Weth, P. Mészáros, T. Kallman, M. J. Rees, *Astrophys. J.* **534**, 581 (2000).
59. M. Böttcher, C. L. Fryer, in preparation (available at http://xxx.lanl.gov/abs/astro-ph/0006076).
60. L. Piro *et al.*, *Science* **290**, 955 (2000).
61. L. Amati *et al.*, *Science* **290**, 953 (2000).
62. M. Vietri, G. Perola, L. Piro, L. Stella, *Mon. Not. R. Astron. Soc.* **308**, L29 (2000).
63. In the supranova scenario (*60*), the interaction of the GRB afterglow with the supernova shell ejected weeks earlier and located about a light day from the burst is envisaged to give rise to Fe recombination lines; this requires in excess of 0.1 to 1 solar masses of Fe in the shell. In a decaying magnetar model (*67*), a long-lived (≳1 day) magnetar or accreting BH with a continuing but decaying jet interacts with the expanding stellar envelope to produce Fe recombination lines, requiring only a normal Fe abundance.
64. T. Galama *et al.*, *Nature* **395**, 670 (1998).
65. J. van Paradijs, *Science* **286**, 693 (1999).
66. J. C. Wheeler, in *Supernovae and Gamma Ray Bursts,* M. Livio, K. Sahu, N. Panagia, Eds. (Cambridge Univ. Press, Cambridge, in press) (available at http://xxx.lanl.gov/abs/9909096).
67. M. J. Rees, P. Mészáros, *Astrophys. J.,* in press (available at http://xxx.lanl.gov/abs/astro-ph/0010258).
68. R. Wijers, J. Bloom, J. Bagla, P. Natarajan, *Mon. Not. R. Astron. Soc.* **294**, L13 (1998).
69. T. Totani, *Astrophys. J.* **511**, 41 (1999).
70. A. Blain, P. Natarajan, *Mon. Not. R. Astron. Soc.* **312**, L35 (2000).
71. S. Mao, H. J. Mo, *Astron. Astrophys.* **339**, L1 (1998).
72. D. Q. Lamb, D. Reichart, *Astrophys. J.* **536**, L1 (2000).
73. R. Perna, A. Loeb, *Astrophys. J.* **508**, L135 (1998).
74. A. Loeb, R. Barkana, *Annu. Rev. Astron. Astrophys.,* in press (available at http://xxx.lanl.gov/abs/astro-ph/0010467).
75. N. Hayashida *et al.*, *Astrophys. J.* **522**, 225 (1999).
76. E. Waxman, *Phys. Rev. Lett.* **75**, 386 (1995).
77. C. Dermer, in preparation (available at http://xxx.lanl.gov/abs/astro-ph/0005440).
78. E. Waxman, J. N. Bahcall, *Phys. Rev. Lett.* **78**, 2292 (1997).
79. J. Rachen, P. Mészáros, *Phys. Rev. D* **58**, 123005 (1998).
80. E. Waxman, J. N. Bahcall, *Phys. Rev. D* **59**, 023002 (1999).
81. F. Halzen, *17th International Conference on Weak Interactions and Neutrinos* (available at http://xxx.lanl.gov/abs/astro-ph/9904216).
82. E. V. Derishev, V. V. Kocharovsky, Vl. V. Kocharovsky, *Astrophys. J.* **521**, 640 (1999).
83. J. N. Bahcall, P. Mészáros, *Phys. Rev. Lett.* **85**, 1362 (2000).
84. P. Mészáros, M. J. Rees, *Astrophys. J.*, in press (available at http://xxx.lanl.gov/abs/astro-ph/0007102).
85. R. Atkins *et al.*, *Astrophys. J.* **533**, L119 (2000).
86. N. Gehrels, P. Michelson, *Astropart. Phys.* **11**, 277 (1999).
87. L. S. Finn, S. Mohanty, J. Romano, *Phys. Rev. D* **60**, 121101 (1999).

88. Supported by NASA grants NAG5-9192 and NAG5-9153 and by NSF grant PHY94-07194.

REVIEW

Magnetohydrodynamic Production of Relativistic Jets

David L. Meier,[1]* Shinji Koide,[2] Yutaka Uchida[3]

A number of astronomical systems have been discovered that generate collimated flows of plasma with velocities close to the speed of light. In all cases, the central object is probably a neutron star or black hole and is either accreting material from other stars or is in the initial violent stages of formation. Supercomputer simulations of the production of relativistic jets have been based on a magnetohydrodynamic model, in which differential rotation in the system creates a magnetic coil that simultaneously expels and pinches some of the infalling material. The model may explain the basic features of observed jets, including their speed and amount of collimation, and some of the details in the behavior and statistics of different jet-producing sources.

A jet is a tightly collimated stream of fluid, gas, or plasma. It typically carries kinetic and internal energy and linear momentum, and if it is set spinning about its direction of motion by some means, it can carry angular momentum as well. A relativistic jet is one whose speed approaches the universally constant speed of light c = 299,792.5 km s^{-1}. At such velocities, Einstein's theory of relativity becomes important. The kinetic energy of motion (and possibly the internal thermal and magnetic energy as well) adds mass to the jet, equal to E_{kinetic}/c^2, making it more difficult to accelerate. Also, as seen by viewers at rest, time slows down in the moving jet material, and any light or radio emission from the jet tends to be radiated in the direction of flow, not isotropically, as would be the case if the flow velocity were subrelativistic. Because c is a maximum speed limit and because conditions become more extreme as it is approached, the Lorentz factor

$$\Gamma = \left(1 - \frac{v^2}{c^2}\right)^{-1/2} \quad (1)$$

is often used to characterize the speed, rather than the velocity v. For example, Γ = 10 describes a flow at 99.5% of c, with each particle in the jet having a mass 10 times as much as it has when it is at rest.

For analyzing observations of relativistic jets, the Doppler factor

$$D = \left[\Gamma\left(1 - \frac{v}{c}\cos\theta\right)\right]^{-1} \quad (2)$$

is an equally important parameter; θ is the angle between the jet flow direction and the observer's line of sight. For low-speed jets with $v \ll c$, this reduces to the familiar nonrelativistic Doppler factor $D \approx 1 + (v/c)\cos\theta$ that is responsible, for example, for the slight frequen-

[1]Jet Propulsion Laboratory, California Institute of Technology, Pasadena, CA 91109, USA. [2]Faculty of Engineering, Toyama University, Gofuku 3190, Toyama 930-8555, Japan. [3]Physics Department, Science University of Tokyo, Shinjuku-ku, Tokyo 162, Japan.

*To whom correspondence should be addressed. E-mail: David.L.Meier@jpl.nasa.gov

cy shift of spectral lines in binary stars as they approach or recede. The relativistic Doppler factor describes both the time dilation effect, which is present even when the jet motion is perpendicular to the line of sight ($\theta = \pi/2$), and the effects of Doppler boosting and focusing. A jet emitting at a single spectral color, for example, would appear to be emitting at a frequency D times higher and into a solid angle D^2 times smaller—a combined factor of D^3 times brighter if moving toward us. If moving away ($\theta > \pi/2$), the jet would be fainter, because D would be <1.

Relativistic Astrophysical Jets

Relativistic jets are common in the astrophysical environment. Objects known or suspected to produce them include the following.

Radio galaxies and quasars. The extragalactic radio sources produce by far the largest and most energetic jets in the universe, although they do not produce the fastest ones nor those with the highest instantaneous powers. The measured speeds of extragalactic radio jets range from $0.1c$ to $\Gamma \approx 20$ and perhaps higher (*1*). The less luminous ones appear as giant elliptical radio galaxies (Fig. 1), and the most luminous appear as radio quasars, generating up to 10^{46} erg s^{-1} or more of power. Often, the twin jets are pointed at a large angle to our line of sight, allowing the full extent of the radio source powered by the jet—up to a few megaparsecs in size—to be seen. In a few sources, however, one of the jets points nearly directly toward Earth and the other points nearly directly away. The approaching jet therefore appears to be substantially Doppler brightened, and the receding one may be so Doppler dimmed that it is difficult or impossible to detect.

The plasma in these jets contains high-energy electrons, trapped in a magnetic field, that emit primarily radio synchrotron radiation, but are detectable in optical synchrotron if the source is close enough. Discovered a century ago, the jet in the galaxy Messier 87 (M87) (Fig. 1), for example, has shown motion with a Lorentz factor of up to ~6 and is pointed at $\theta < 19°$ to our line of sight (*2*). At the center of M87 lies a supermassive black hole, $\sim 3 \times 10^9 M_\odot$ (solar masses) in size (*3*), that is thought to be the heart of the engine responsible for generating the jet. Black holes of 10^6 to $10^{10} M_\odot$ are, in fact, thought to power nearly all types of active galactic nuclei (AGN), including radio galaxies, radio quasars, radio quiet quasars, and Seyfert galaxies. Why some of these objects appear to have produced jets nearly continuously for tens of millions of years or longer, whereas others have been jet-quiet for an equally long time, is one of the major scientific questions in this field.

Microquasars. Although the supermassive quasars lie at the centers of galaxies and are fed by ambient stars and gas that collect there and accrete into the black hole, there also are much lower mass versions of these, scattered about the Milky Way Galaxy and fed by the stripping of atmospheric layers from a single companion star. A few of these binary x-ray sources, called microquasars, produce jets (*4*). There are two basic types of microquasar: one whose central engine is powered by a black hole of $\sim 10 M_\odot$ and one that is powered by an even lower mass object, a neutron star of only $\sim 1.4 M_\odot$. In the latter case, the jets can be moderately relativistic, $0.26c$ for the twin-jet star SS 433, for example (*5*). In the black hole cases, the jet speeds reach $\Gamma \sim 2.5$ ($0.92c$). So far, a microquasar with a Lorentz factor of 10 to 20 has not been seen. This just may be due to small-number statistics: the number of high-Γ microquasars in our Galaxy may be small already, and it is unlikely that Earth lies within the small-emission solid angle of any one of these. Because the time scale for events to happen near accreting black holes is directly proportional to the mass of the hole, microquasars offer the possibility of watching a quasar-like object evolve through many stages of its life in a few years or decades rather than waiting the millions of years necessary for the extragalactic objects to change.

Supernovae. There is now evidence that supernovae, especially those that are not surrounded by a large red giant envelope, explode in a decidedly aspherical manner (*6*). Theoretical and observational studies point to the possibility that the asymmetry could be caused by the ejection of twin jets from the central core of the supernova as it collapses to form a hot neutron star (*7*). The speed of such a jet would be about the escape speed from the proto–neutron star ($0.25c$ to $0.6c$). Even if only a small fraction of the core were ejected in the jet (e.g., ~1%), it would have enough kinetic energy to substantially alter the structure of the expanding supernova shell, if not in fact to provide much of the observed explosive power of 10^{51} to 10^{52} ergs in a few seconds of time.

Gamma-ray bursts. Gamma-ray bursts (GRBs) provide perhaps the most extreme example of relativistic flow that may be a jet, exhibiting speeds of $\Gamma \sim 100$ or more. Although GRBs may be associated with supernovae in some cases, they are a million times rarer than classical supernova events (*8*). If only those events are observed that are within an angle $\theta \sim \Gamma^{-1}$ of our line of sight, then there could be 10^4 more events Doppler boosted in directions other than ours, bringing the GRB rate to within a factor of 100 or so of the supernova rate and their derived explosive energies down to $\sim 10^{52}$ to 10^{53} ergs, about the same as that of powerful supernovae. The high Lorentz factors and energies are consistent with the catastrophic formation of a stellar mass black hole of $\sim 10 M_\odot$, with ~1% going into a jet outflow. This could be the extreme example of the jet-producing supernova discussed above, in which instead of halting at the neutron star

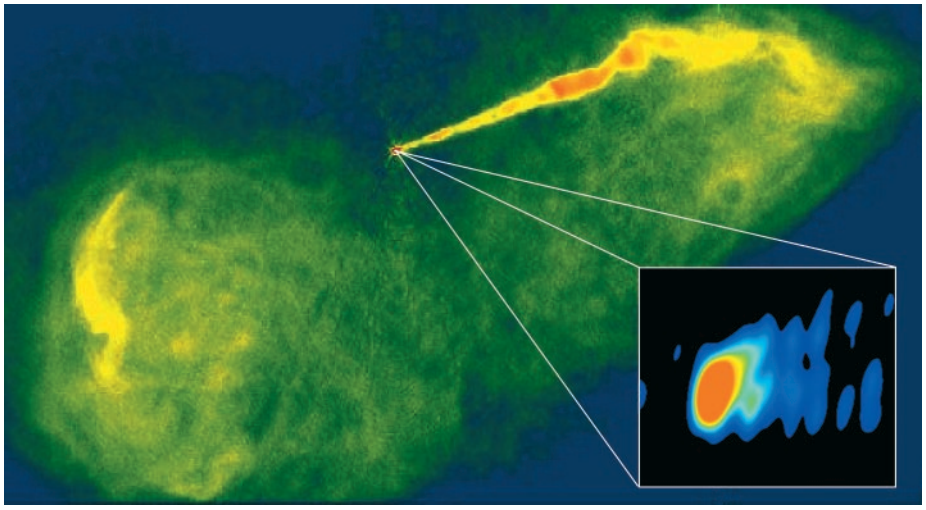

Fig. 1. The jet in the galaxy M87 displays most of the important features of relativistic jets. The approaching northwest jet is Doppler boosted, whereas the southeast one is virtually undetectable because it radiates away from Earth. The lobes, consisting of decelerated jet material, radiate isotropically, and therefore both are visible. The full extent of the source projected on the sky in this image is ~80 arc sec or 6 kpc. Because the source is at an angle of $<19°$ to our line of sight, its deprojected length must be at least 20 kpc. Deep in the core (inset), the jet shows an initial wide opening angle (60°) that decreases with distance from the core. This indicates that the acceleration and collimation region may be resolved. The length of the jet emission in the inset is ~0.001 arc sec or 16,000 astronomical units, which is only ~250 times the Schwarzschild radius of the central $3 \times 10^9 M_\odot$ black hole. [Images were made with the National Radio Astronomy Observatory's Very Large Array and Very Long Baseline Array and are courtesy of J. Biretta and W. Junor; reprinted by permission from *Nature* (*37*) copyright (1999) Macmillan Magazines Ltd.]

stage, the collapse continues to the black hole stage, producing an even faster jet in the process. Other scenarios, such as the merger of two neutron stars, could trigger a similar event.

In all observed cases of relativistic jets, the central object is compact, either a neutron star or black hole, and is accreting matter and angular momentum. In addition, in most systems there is direct or indirect evidence that magnetic fields are present (detected in the synchrotron radiation in galactic and extragalactic radio sources or inferred in collapsing supernovae cores from the association of remnants with radio pulsars). This combination of magnetic fields and rotation may be responsible for the observed relativistic jets.

Basic Physics of Magnetohydrodynamic Acceleration and Collimation

Although several different methods of producing and collimating jets have been proposed, the leading model is the magnetohydrodynamic (MHD) model. It potentially can account for jet collimation and acceleration to relativistic velocities while operating within the gravitational collapse and/or accretion paradigms for jet-producing sources. In addition, the model suggests a trigger mechanism for some GRBs, a way of producing the most powerful quasar jets observed as well as the difference between radio loud and radio quiet quasars, and an explanation for the detailed changes that occur in microquasar jets as their accretion disks change their structure.

The flow of a magnetized plasma is most generally described by kinetic theory, general relativity, and Maxwell's equations for the electromagnetic field. However, many of its features are captured by making two simplifying assumptions: The plasma particles act like a fluid and the conductivity is so high in the plasma that electric fields generated by free charges are shorted out. Both of these assumptions (which describe the astrophysical plasmas of interest) give rise to the field of study of ideal magnetohydrodynamics. Although the equations are still complex in nature, the differences between regular fluid flow and ideal MHD flow can be understood from the following discussion and from Fig. 2, which shows a three-dimensional MHD jet propagation simulation (*9*). Under these assumptions, the magnetic field lines thread the plasma and are tied to it (frozen in). These field lines have three important properties. First, to a good approximation, plasma cannot cross the field lines; it can only flow parallel to them. If the field is strong (i.e., if the hydrodynamic pressure of the plasma ρv^2 is less than the magnetic pressure $B^2/8\pi$, where ρ is the plasma mass density, v is its velocity, and B is the magnetic field strength) and if it is anchored in a rotating star or disk, then any plasma trapped in the field will be flung centrifugally outward along the field lines. On the other hand, if the field is weak or the plasma is dense, then the rotating field will be bent backward in a sweeping spiral. Second, parallel magnetic field lines tend to repel each other. This produces a partial pressure on the plasma perpendicular to the field lines, but not parallel to them, due solely to the field. A weak field can be strengthened by bringing together many weak parallel lines of force to produce the equivalent of a few strong ones. Thus, compression perpendicular to the field lines or toroidal coiling around an axis for many turns can enhance the field, increasing its pressure and energy density. Third, magnetic field lines do not maintain a curved shape unless they are acted on by forces from the plasma or other field lines. Left alone, they tend to straighten like springy wires. If coiled in a hoop or spiral, the field will try to shrink around its axis to eliminate all but the straight axial component of the field. This hoop stress is responsible for the well-known pinch effect of plasma physics and for the collimation of relativistic jets.

To accelerate and collimate a jet with magnetic fields, all that is needed is a gravitating body to collect the material to be ejected, a poloidal magnetic field threading that material, and some differential rotation (Fig. 3). The differential rotation produces a magnetic field helix about the rotation axis. This rotating field coil then drives the plasma trapped in it initially upward and outward along the field lines as they try to uncoil. As this twist propagates outward, the toroidal field pinches the plasma toward the rotation axis. Depending on the relative importance of the magnetic field, plasma density, and rotation, a variety of results are possible, such as a broad uncollimated wind, a slowly collimating bipolar outflow, and a highly collimated jet.

The physics of jet production can be an-

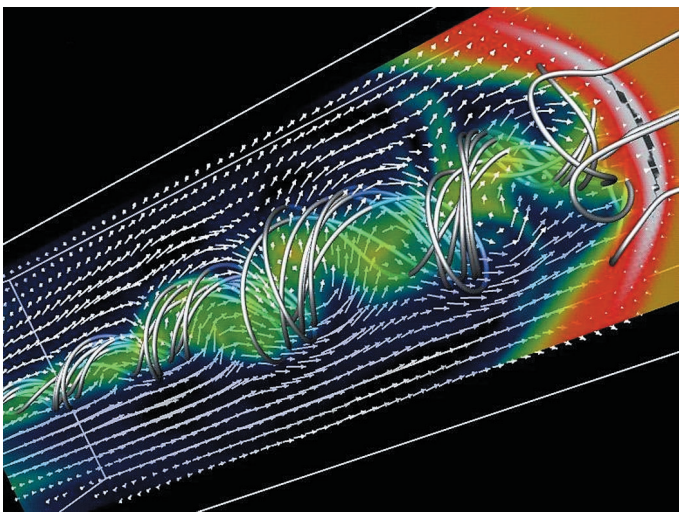

Fig. 2. A three-dimensional simulation of the propagation of a magnetized jet, which depicts most of the properties of the MHD model. The diagram shows flow velocity (arrows), the plasma density field (color, with white and blue indicating high and low pressure, respectively), and the magnetic lines of force (metallic tubes). The initially axisymmetric, rotating jet has developed a helical-kink instability that distorts its shape. The plasma flow still follows the field lines. Such an instability may explain the wiggles observed in some parsec-scale radio jets. The super–Alfvénic jet terminates in a strong shock wave at right, as it propagates into a region with decreasing Alfvén velocity. High-energy particles accelerated in the rotating magnetic twists, and especially in the compressed field behind the bow shock, will emit synchrotron radiation. This shock therefore may correspond to the hot spot often seen at the end of jets in many radio sources. [Courtesy of M. Nakamura]

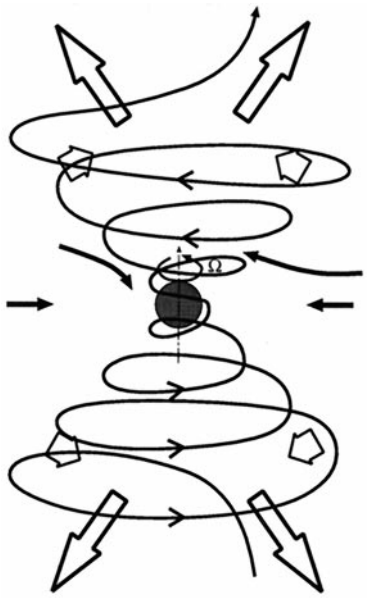

Fig. 3. Schematic diagram depicting the MHD acceleration and collimation model. Magnetized and rotating inflow toward a compact object (solid arrows) winds the magnetic field lines into a rotating helical coil called a torsional Alfvén wave train (TAWT). Magnetocentrifugal forces expel some of the material along the field lines and magnetic pressure and pinching forces (short open arrows) further lift and collimate it into a jet outflow (long open arrows).

alyzed by comparing time scales on which different processes occur. In this case, the most important time scale is the dynamical time τ_d, which is the characteristic time for information to propagate through the system. In a magnetized plasma, $\tau_d = R_0/c_{ms}$, where the magnetosonic sound speed c_{ms} includes both plasma and magnetic field pressure and R_0 is the characteristic size of the jet-production region. Because the system is initially in equilibrium and confined by gravity, the dynamical time is comparable to the free-fall or escape time $\tau_{esc0} = (R_0^3/2GM)^{1/2}$ (which is a constant factor $1/2^{3/2}\pi = 0.11$ shorter than the orbital period at R_0), where M is the mass of the central object and G is the gravitational constant.

The response of a jet-producing system to the twisting of the magnetic field depends on the time it takes for the magnetic energy to, say, double. If this takes longer than a dynamical time, then the system's internal structure can adjust in a quasi-static fashion to accommodate the new conditions. However, if the increase occurs in less than a dynamical time, then the new conditions surprise the system, forming shock waves that distribute the new information in less than a sound-crossing time. Often, such rapid changes in the system result in a catastrophe, such as an explosion or a collapse. Determining which type of jet outflow results and finding what its effects are on the jet-producing system are some of the chief goals of the study of MHD jet production.

Astrophysical Applications of the MHD Mechanism

One of the earliest applications of the MHD model was pulsar wind theory, developed to explain observations of the Crab Nebula (*10, 11*). The observations showed that a large amount of particle energy was being injected continually into a supernova remnant, probably from the pulsar at the center of the nebula. Because the magnetic fields near a pulsar are very strong ($B^2/8\pi \gg \rho v^2$) and the particle density is low, radial outflow was expected, not a collimated jet. Therefore, work on pulsar winds tended to focus on accelerating the particles and feeding the nebula. Much later, however, the twin-jet star SS 433 was discovered, which may be a pulsar buried in a dense accreting envelope (*5, 12*). This object is probably an example of the opposite extreme: as the dense material falls toward the neutron star, it bends the pulsar magnetic field backward, producing a tight helical coil that results in a narrow jet (Fig. 4A). In addition, new images from the Chandra X-ray Observatory now show that even isolated pulsars can produce jetlike structures (*13*).

Also in the late 1960s, and quite independently, investigators studying the late stages of stellar evolution performed computer simulations of the effects of a magnetic field on the collapse of a rotating stellar core as it forms a proto–neutron star (*14, 15*). The simulations found that, even if the initial magnetic field were weak, during the core collapse it was enhanced by differential rotation to such large values, in less than a dynamical time, that a magnetic explosion occurred, driving away the stellar layers by magnetic pressure alone, sometimes in a jet along the rotation axis (Fig. 4B). Further studies of this mechanism (*16*) concluded that explosive MHD jets would not occur in most collapsing supernova cores. Instead, over several dynamical time scales, a magnetic bubble would be produced in each of the northern and southern hemispheres and then buoyantly rise up the rotation axis, bursting into the surrounding stellar envelope. Only in a few rare energetic cases would a narrow fast jet form.

Modern MHD jet theory, and its relation to accreting stars and black holes, began in the mid-1970s when it was shown that the same MHD processes occurring in pulsars and collapsing magnetized supernova cores also could occur in magnetized disks in Keplerian rotation about accreting stars and black holes (*17, 18*), as well as near the horizon of the spinning black hole (*19*). In the latter case, the magnetic field extracts energy and angular momentum not from the accreting matter but rather from the black hole's rotation. These two related jet mechanisms are pictured in Fig. 4, C and D.

One way to study these MHD acceleration problems is to set up and solve the full set of eight partial differential MHD equations on a computer, making as few assumptions as possible. Such simulations often run for several hours or days on large supercomputers, calculating the evolution of a rotating disk or stellar core of magnetized plasma and showing the effects of the field on the flow, and the flow on the field. Multidimensional and supersonic processes, such as jets, rotation, and shock waves, can be followed in detail.

With the exception of the early work on MHD supernovae, until the mid-1980s most MHD acceleration models were semi-analytic; that is, by making several simplifying assumptions, the eight MHD partial differential equations were reduced to one ordinary differential equation that could be solved quickly on a modest computer. One of the most widely used assumptions was that of a steady state, in which the plasma flow and magnetic field structure do not change with time. This assumption causes the solution to focus on the long-term structure that forms

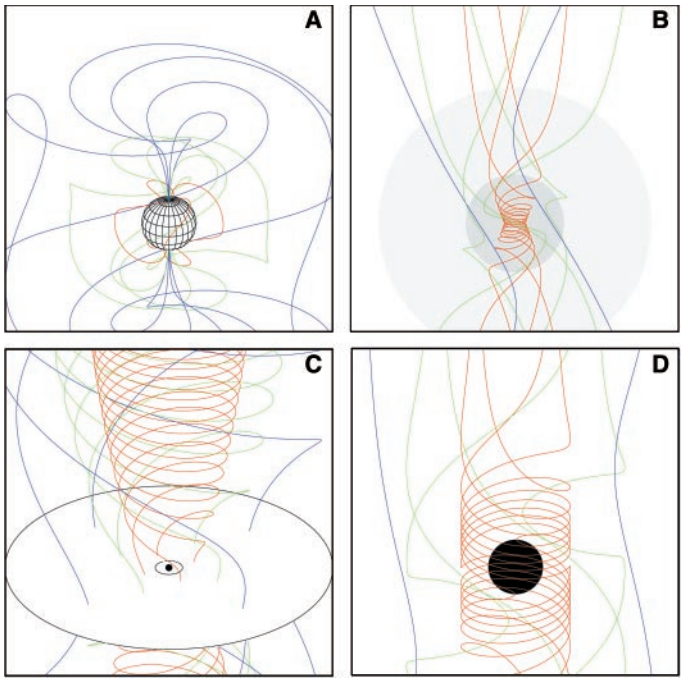

Fig. 4. Schematic diagrams of four astrophysical scenarios in which differential rotation of a magnetic field might generate relativistic jet outflow. Color is used to aid in identification of the field lines. (**A**) The dipole field of a heavily accreting, rapidly rotating pulsar can be swept back by the accreting matter as close as a few tens of kilometers from the stellar surface. Some of this material will be ejected in a jet at the local escape speed. (**B**) A slowly rotating pre-supernova white dwarf or dense stellar core will collapse to a rapidly rotating proto–neutron star. Even an initially uniform axial field will be drawn inward and wound into a tight coil, ejecting some of the dense core material. The jet may have sufficient power to alter the shape of the supernova ejecta or even drive the explosion on its own. (**C**) The poloidal magnetic field protruding from an accretion disk orbiting a compact object will fling disk coronal material outward in a wind. Conservation of angular momentum will slow the wind's rotation and, if the outflow is dense enough, sweep back and coil the field lines. (**D**) Near a rotating black hole, the space itself rotates differentially. This dragging of inertial frames is particularly strong inside a radius about twice that of the hole—the ergosphere—where material must rotate with the hole. Here only the twisting of vertical field lines is shown, but as the plasma accretes toward the black hole, these lines will be drawn inward, creating a structure similar to that in (B) or (C).

after transient effects due to the initial conditions have died away. Other assumptions were made to simplify the geometry of the problem, such as that of self-similarity. This assumes that the structure scales with distance from the compact object, so that it looks similar at every radius. Under these simplifying assumptions, most semi-analytic studies showed that, although MHD winds should form, the acceleration should be slow, and the outflow should occur in a rather broad bipolar structure, not a tightly collimated jet (*20, 21*). The broad structure found from steady-state studies was inconsistent with the narrow jet found in dynamical supercomputer simulations of collapsing supernova cores (*14*).

Semi-analytic studies and numerical simulations provide complementary ways in which jet formation can be investigated. Analytic or semi-analytic studies often ignore the effects of an inner accretion disk boundary, for example, or of a central black hole horizon, and they usually do not treat the time-dependent nature of the flow. On the other hand, because their results are expressed in terms of simple parameters (central object mass, magnetic field strength, etc.), they often are applicable to many different situations. Both approaches are critically dependent on the initial conditions and boundary conditions that are applied. In the case of numerical simulations, these conditions even can cause spurious effects, particularly along boundaries where the plasma should flow out of the computational domain unimpeded. Sometimes the boundary instead reflects waves back into the grid, modifying the flow in an unphysical manner. Such errors are minimized by locating outflow boundaries as far away as possible by progressively increasing the spacing between mesh points beyond the region of interest. When performed and interpreted carefully, numerical simulations have an ability to characterize the two- or three-dimensional structure of the plasma flow and magnetic field that is unequaled by any other technique. The goal is to create a third field of study, complementing observation and theory, in which the computations themselves are sophisticated enough that numerical experiments on them, with computer visualization techniques, can yield insight into the inner workings of astrophysical processes that could not be obtained in any other way.

Dynamical MHD Supercomputer Simulations: Narrow Jets at the Escape Velocity

Numerical simulations of magnetized accretion disks around stars (*22, 23*) and supermassive objects (*24–26*) have shown that a collimated jet, similar to that discovered for collapsing stellar cores, is a general feature of rapidly rotating, gravitationally confined plasmas that are threaded with a magnetic field. A typical simulation of this type, using high-fidelity modern supercomputer and visualization techniques, is shown in Fig. 5.

The simulation begins with a rather thick accretion disk or torus surrounding a point mass at the center. This initial disk is in rotational equilibrium about the central object, producing differential rotation in the radial direction. The torus also is threaded with an axial (vertical) magnetic field of sufficient strength to exert a braking force on the rotating plasma. As the simulation proceeds, the braking force removes angular momentum from the torus, transferring it up along the magnetic field lines and to the coronal plasma (which also is frozen to the field lines), in a large-amplitude torsional Alfvén wave train (TAWT). As these rotating magnetic twists propagate out in bipolar directions along the rotation axis, they push out and pinch the coronal plasma into a slender spinning jet. The loss of angular momentum to the jet allows the disk material to fall toward the central object, with half of the gravitational energy released in this accretion going into additional kinetic energy of rotation that continues to power the TAWT and the accretion. This process is most effective near the surface of the torus, resulting in an avalanche type of accretion in the surface layers.

This sweeping pinch mechanism appears to be nearly universal. It can occur in a collapsing star, above an accretion disk, or near a rotating black hole. In a few dynamical times, a differentially rotating magnetic field can produce twin tightly collimated jets along the rotation axis from what would otherwise have been only a flattened system. The two jets carry away angular momentum and rotational energy and, if not exactly balanced in linear momentum, also may impart a thrust to the accreting object.

Apart from the collimation itself, perhaps the most interesting parameter determined by these simulations is the speed of the ejected jet. In most simulations performed, the jet speed is close to the escape speed as measured at the base of the jet (*27*). For all stars for which the rotation is nonrelativistic, including nonrotating black holes, the escape speed is given by $v_{esc0} = (2GM/R_0)^{1/2}$. In the more general case of rotating black holes, the escape Lorentz factor (given by the inverse of the gravitational lapse function) is

$$\Gamma_{esc0} = \left\{ \frac{\left[1 + \left(1 + 2\frac{R_g}{R_0}\right)\left(j\frac{R_g}{R_0}\right)^2\right]}{\left[1 - 2\frac{R_g}{R_0} + \left(j\frac{R_g}{R_0}\right)^2\right]} \right\}^{1/2} \quad (3)$$

where $R_g = GM/c^2$ is the gravitational radius of the black hole (one-half the Schwarzschild radius) and $j = J/J_{max}$ is the black hole angular momentum normalized to the maximum possible value, $J_{max} = GM^2/c$. When $j = 0$, Eqs. 1 and 3 reduce to the familiar expression for v_{esc0}.

Fully general relativistic simulations of jet production have been performed for accretion

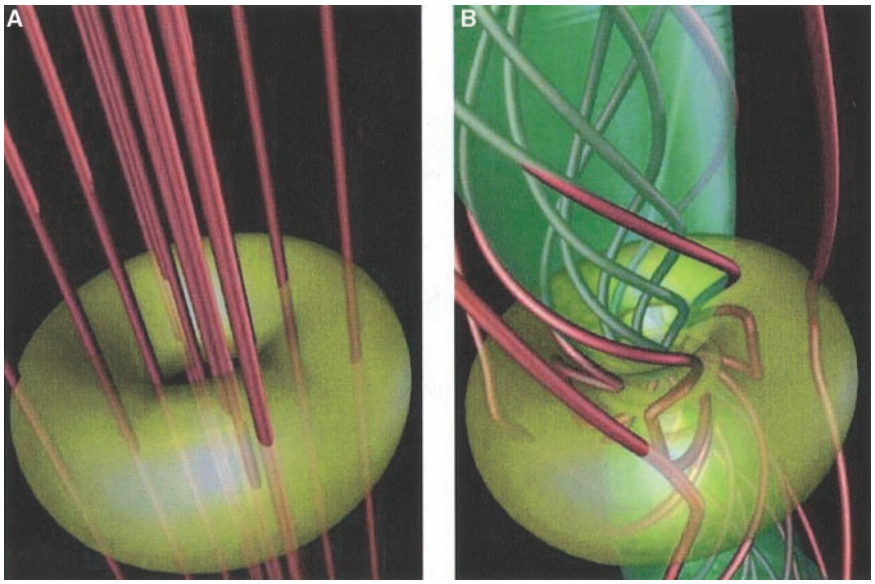

Fig. 5. An MHD simulation of a thick magnetized torus surrounding a supermassive (10^8 $M_\odot$) central object (*26*). (**A**) Initial state showing the torus in rotational equilibrium with an axial magnetic field. (**B**) As the simulation begins, the differentially rotating torus drags the field lines in the azimuthal direction, creating a braking force that allows the material to accrete inward and gain additional rotational energy. The effect of this process is to produce a torque on the external magnetic field, generating a torsional Alfvén wave and a spinning plasma jet that carries away matter, angular momentum, and energy from the system. Far above the disk, the torsional waves will be unstable to the helical-kink instability, generating the wiggled structure seen in Fig. 2.

disks around both nonrotating (Schwarzschild) black holes with $j = 0$ and rotating (Kerr) holes with $j = 0.95$ (*28–31*). In the Schwarzschild case (Fig. 6A), the radius of the inner edge of the accretion disk is about equal to that of the last stable orbit ($6R_g$), making the jet-production region around $R_0 = 7R_g$ to $8R_g$ in size. In the Kerr case (Fig. 6B), stable orbits exist nearly down to the horizon at $1.31R_g$, so R_0 must be of order of the radius of the ergosphere ($R_e = 2R_g$). The ergosphere is the region surrounding a rotating black hole, inside of which accreting material must rotate in the same direction as the black hole rotates. From Eq. 3, we expect jet speeds of about $\Gamma_{esc0} = 1.18$ and 2.54 ($v_{esc0} = 0.53c$ and $0.92c$, respectively). This is confirmed by the simulations in Fig. 6.

In the Schwarzschild case, the jet is driven by the orbital motion of the accretion disk around the black hole. In the Kerr case, however, although we gave the disk no initial rotation, a powerful $\Gamma > 2$ jet still formed. The reason is that, as the accreting matter plunged into the ergosphere, it became caught up in the rotating space around the black hole (Fig. 4D). This rotation with respect to the outside material created a sweeping pinch in a manner similar to that in the orbiting disk case. The jet was driven not by any intrinsic rotation in the disk but by the rotation of the black hole itself.

In all the above simulations, the process of accreting the inner disk, winding the field, and ejecting the jet is a dynamical one, occurring in one or two rotation times. However, it is not necessarily a transient one. If accreting material and the magnetic field are continually supplied from the outer region of the disk at a rate comparable to that falling into the hole plus that ejected by the jet, then the system will reach a steady state in which a jet is continuously produced. On the other hand, if the disk is depleted by the rapid accretion and jet at a rate faster than it is replenished from the outside, then the jet will cease and begin again only after the disk refills.

Steady-State Simulations: Broad Jets at the Escape Velocity

The above model works as long as the assumption of a magnetic field frozen into the plasma remains valid. This certainly will be the case when the infall rate is close to the free-fall rate, as it is in the above simulations. However, if the rate at which the magnetic field is being dragged inward by the accretion inflow is slower than the rate at which it diffuses outward against that flow, then the field in and above the disk at a given radius will be determined mainly by local turbulent dynamo processes generating that field. Inflow of magnetic field will be negligible. This probably will be the case when the disk is in Keplerian rotation and the inflow velocity is a factor of 10 or more smaller than the free-fall rate. Because one wants to avoid the complications of the internal dynamo processes in the disk, to simulate this opposite extreme case, it is frequently assumed that the disk is infinitely thin along the equatorial boundary and continuously boiling off material into poloidal magnetic field lines that are embedded in it (*32–34*). Although these simulations begin with an initial disk corona configuration, they are typically run for very long times (1000 dynamical times or more) until that initial configuration has been expelled by the MHD wind from the disk. At this point, the magnetic field structure and plasma flow cease to change with time and the system reaches a steady state, just as assumed in the early semi-analytic studies of MHD acceleration. The resulting structure will be a function of the boundary conditions only and not the initial conditions.

The process of jet formation in this case is similar to that in Figs. 5 and 6, but the means of inducing differential rotation is different. The matter injected from the disk boundary is initially flung outward along the field lines; conservation of angular momentum in that material then bends back the field into a spiraling coil that eventually lifts and collimates the flow along the rotation axis. This process is depicted schematically in Fig. 4C, and a numerical simulation of it is shown in Fig. 7. As suggested by the earlier semi-analytic studies (*20*), the acceleration is smoother and the collimation is slower than in the dynamical sweeping pinch. The speed steadily increases along the outflow until it exceeds the local escape velocity, the local poloidal Alfvén speed ($v_{Ap} = B_p/(4\pi\rho)^{1/2}$, where $B_p = (B_R^2 + B_Z^2)^{1/2}$ is the combined poloidal field strength in the cylindrical radial (R) and axial (Z) directions and ρ is the plasma mass density), and finally the local total Alfvén speed v_{At}, which includes the toroidal component B_ϕ (Fig. 7). v_{At} is the speed with which magnetic waves travel along the twisted field. The jet eventually collimates and reaches a speed of order v_{esc0}, but this does not occur until well above the disk. There is a large region (perhaps 100 R_g or so in size in the black hole case) where the flow is rather broad.

The numerical simulations suggest that, when a jet-producing system enters an active dynamical phase, it should generate tightly collimated jets that may be time dependent. On the other hand, more quiescent sources should pro-

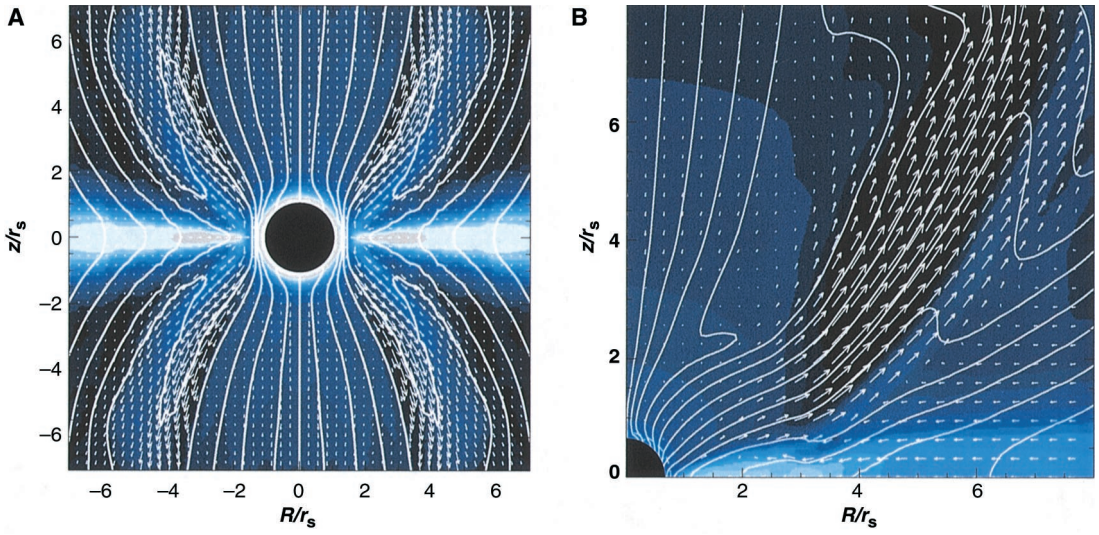

Fig. 6. Two fully general relativistic simulations of jet production by accretion disks around black holes. Each begins with an axial field. Plots are meridional cuts, with length units in Schwarzschild radii ($2R_g$), and show the plasma density in blue-white color, poloidal velocity vectors with white arrows, and a poloidal magnetic field as solid white lines. (**A**) A nonrotating, Schwarzschild hole with a moderately strongly magnetized Keplerian disk whose rotation drives an MHD jet at the escape speed (~0.4c) [from (*28*)]. (In this simulation, a gas-pressure-driven outflow also is ejected from a radius interior to the last stable orbit at a somewhat higher speed.) (**B**) A rotating Kerr hole ($j = 0.95$) (in the lower left corner) with a nonrotating disk [from (*30*)]. Preliminary analysis indicates that the dragging of inertial frames drives the jet from a region just outside the ergosphere at $R \sim 1r_S$ to $2r_S$ ($2R_g$ to $4R_g$) at the escape speed of $\sim 0.93c$ ($\Gamma \approx 2.7$).

duce steady-state flows that collimate more slowly. Observations of some microquasars and radio galaxies lend support to this model. The microquasar GRS 1915+105 often undergoes bright unsteady outbursts, in which the x-ray luminosity reaches close to the limit established by Eddington for radiation pressure on free electrons. During these outbursts, the inner disk exhibits cyclic behavior, firing off a jet every 12 to 60 min, as the disk is emptied by the jet and then refilled by accretion (*35*). However, after a major outburst subsides, GRS 1915+105 enters a quiescent phase that lasts for several days. About 18 hours after the beginning of this phase, a steady weak jet appears and remains until the next outburst (*36*). So the source produces transient jets when it is bright and dynamic and a steady jet when it is in quiescence.

In addition, high-resolution images of the core of the radio galaxy M87 at 43 GHz (*37*) may have resolved the jet-collimation region in the source and show a possible broad flow that collimates slowly (Fig. 1). The radio power of this galaxy is rather weak (10^{41} erg s^{-1}) for the mass of its black hole (3×10^9 $M_\odot$). Both its possible broad collimation region and its weak jet power, therefore, are consistent with it being in a steady state like that depicted in Fig. 7.

Finally, the steady-state calculations may describe the behavior of a newly formed pulsar just after collapse of the supernova core. A recent reanalysis of the collapsing supernova core problem (*38*) shows that, after the collapse halts, the proto–neutron star enters a deleptonization phase in which its radius shrinks from 50 to 10 km as it emits neutrinos. This phase should last 5 to 10 s, which is $>10^4$ dynamical times. This is enough time for the many buoyant bubbles produced to merge into a steady, slowly collimating bipolar flow along the rotation axis (Fig. 7). The energy and momentum in the flow should cause an already-occurring supernova explosion to be aspherical. Furthermore, although still controversial, this MHD outflow in fact could be the deciding factor in assisting a supernova explosion that otherwise would have failed (*7*).

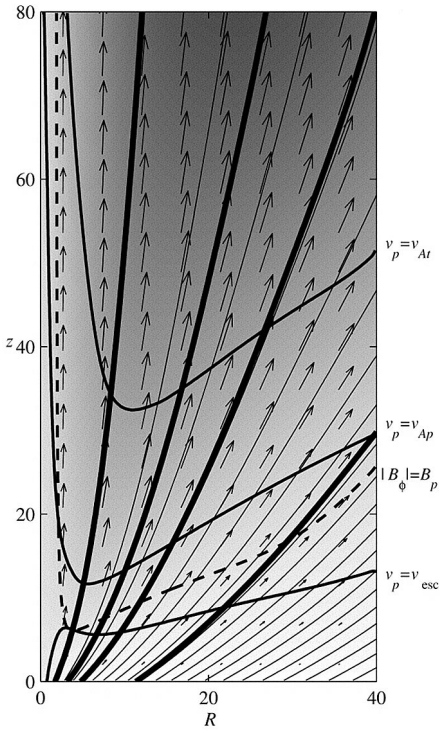

Fig. 7. An accretion disk wind in a steady state [from (*34*) and similar to results in (*33*)]. The central object is at (0, 0), and the infinitely thin disk is along $Z = 0$. Arrows indicate velocity vectors. Lines anchored in the disk and arching upward are contours of magnetic flux; the dashed curve indicates the surface above which the strength of the azimuthal (B_ϕ) component of the twisting magnetic field exceeds the poloidal field strength [$B_p = (B_R^2 + B_Z^2)^{1/2}$]; and the three labeled curves show surfaces where the poloidal velocity achieves the escape velocity, the poloidal Alfvén velocity (determined by the poloidal field alone), and the total Alfvén velocity. Any transient properties of the flow have disappeared, leaving a slowly accelerating bipolar wind that collimates from opening angles of ~40° to 50° to only a few degrees over many tens of inner disk radii. Such a picture is qualitatively and, perhaps, quantitatively similar to the wide opening angles observed in M87 in the inner core (Fig. 1). [Figure courtesy of R. Krasnopolsky]

The Steady-State Strong-Magnetic-Field Case: Fast and Narrow Jets

Ejection of jets at the local escape speed may be able to explain the jet speeds observed in microquasars and those in radio galaxies and quasars with $\Gamma \lesssim 3$. This model even offers suggestions on how jets might arise in collapsing supernova cores to effect asymmetry in the ejecta and perhaps even assist in driving the ejection itself. However, jets propelled at the escape velocity, even from the vicinity of black holes, have a difficult time explaining the Lorentz factors of 10 to 20 seen in the most powerful quasars, and they cannot explain the $\Gamma > 100$ outflow seen in GRBs. Even for a maximal Kerr hole ($j = 0.998$), $\Gamma \sim 10$ to 20 requires that most of the jet be ejected from a region only $1.12R_g$ to $1.21R_g$ in radius, and $\Gamma > 100$ requires that it occur within a mere ~0.2% of the horizon at $1.063R_g$. The need for such contrived scenarios, which so far are not borne out by the numerical simulations of black hole accretion, motivates us to look for another mechanism to achieve high Lorentz factors.

One method of increasing the jet speed in the MHD model is to increase the strength of the magnetic field accelerating the jet and/or reduce the density of the material loading the field lines. This will result in a higher Alfvén speed, which ultimately will produce a higher terminal jet speed. The range of parameter space where high jet speeds are expected is determined as follows. The MHD power is given by (*19*)

$$L_{MHD} = B_{p0}^2 R_0^4 \Omega_0^2 / 32c \qquad (4)$$

It depends only on the poloidal magnetic field B_p protruding from the jet-production region at radius R_0 and on the angular velocity of that field Ω_0. If ρ_0 is the plasma density there, then we define the critical power to be that given by the energy needed for the plasma to reach escape speed divided by the dynamical (free-fall) time

$$L_{crit} = 4\pi\rho_0 R_0^2 \left(\frac{GM}{R_0}\right)^{3/2} \qquad (5)$$

For example, if the central object rotates at the Keplerian rate, then the criterion $L_{MHD} \gtrsim L_{crit}$ is equivalent to having an Alfvén velocity greater than the escape speed ($v_{A0} \gtrsim v_{esc0}$ or $B^2/8\pi \gtrsim \rho v_{Kepler}^2$).

There are two extremes in this high-magnetic-power case: efficient and inefficient acceleration. Compared to the steady-state, weak-field case, these cases correspond to, respectively, rapid acceleration that reaches terminal speed much nearer the black hole and slow acceleration in which the terminal speed is achieved much farther from the hole. If the efficiency of conversion of MHD power to kinetic power is high near the central object (~50%), then the acceleration of the jet material to its terminal speed will occur in a time shorter than τ_{esc0} and within a radius R_0 of the central object. The final kinetic power $L_k = \Gamma \dot{M}_{jet} c^2$ will equal $0.5L_{MHD}$, where $\dot{M}_{jet}$ is the rate of mass outflow in the jet, with the other 50% being mostly in Poynting flux—the energy carried by the torsional Alfvén waves generated by the rotating twisted magnetic field. Solving for the Lorentz factor gives an equipartition Lorentz factor of $\Gamma_{eq} = (v_{A0}^2 R_0^2 \Omega_0^2)/(32c^3 v_0)$. If the speed v_0 at which the plasma is boiling off the disk is small compared to the Alfvén and orbital speeds, which are nearly c if the central object is a black hole, then, potentially, Γ_{eq} can be much larger than unity. A numerical simulation of efficient acceleration in an accretion disk corona for the high-magnetic-power case is shown in Fig. 8. Although this is a nonrelativistic simulation, extrapolation of this result indicates that Lorentz factors of 10 to 20 may be possible (*39*). The jet reaches the equipartition speed, and the high magnetic field strength produces tight collimation of the jet near the accretion disk.

On the other hand, if the acceleration efficiency is well below 50%, then almost all of the power will be in Poynting flux in the TAWT (*40–42*). In that case, the jet terminal speed should be on the order of the Alfvén speed, which will be much higher than v_{esc0} for sufficiently low plasma density and high field strength, and it will be potentially highly

relativistic (*21*). So far, however, numerical simulations of this case have produced jets with speeds well below the Alfvén speed. This is probably because the Alfvén point lies so far from the central object that it has not been included yet in the computational domain (the area of space being simulated). Relativistic simulations that include the Alfvén point should be able to achieve the expected factor of $\Gamma > 10$. An important result from the present numerical simulations of Poynting flux–dominated jets, which was not predicted by the semi-analytic steady-state studies, is that these jets are highly collimated, like the strong-field cases above and unlike the steady weak-magnetic-field case. Therefore, because of the strong pinch that develops, a narrow jet that delivers its thrust in a narrow solid angle may be a general feature of strong rotating magnetic fields ($L_{\rm MHD} \gtrsim L_{\rm crit}$), not only for accretion disks but also perhaps for many jet-producing objects.

A Magnetic Trigger for Some GRBs?

A particularly interesting, though still somewhat preliminary, application of these narrow jets is in the case of collapsing stellar cores. The condition $L_{\rm MHD} \gtrsim L_{\rm crit}$ also may result in a narrow jet in this situation, similar to the results of LeBlanc and Wilson (*14*). In their simulation, the magnetic field grew to a dynamically important value in less than a dynamical time, which is the condition for forming explosive MHD jets in collapsing supernova cores (*16*). However, this is the same condition for a strong magnetic field. So, although most rotating magnetized proto–neutron stars with low MHD power ($L_{\rm MHD} < L_{\rm crit}$) should produce broad slowly collimating jets in a steady or quasi–steady state, a few high power ones should produce narrow fast jets, with the outflow possibly lasting many dynamical times. Although carrying more power, this highly collimated jet will be much less efficient in imparting energy and momentum to the outer stellar layers than a broad bipolar flow (*7*).

This suggests that, because of their broader outflow, cores with low-power MHD outflows should be more efficient at producing asymmetry in their supernova ejecta, whereas the high-power ones should be less efficient in doing so. Furthermore, if MHD outflows from the core are a necessary component in supernova explosions, then those few cores with $L_{\rm MHD} \gg L_{\rm crit}$ may not explode. They may act similarly to the failed supernova model for GRBs, continuing to accrete much of the surrounding stellar layers and collapse to a black hole. This continued collapse has the potential for producing an even faster and narrower jet, just outside the forming and expanding black hole horizon, which could overtake the precursor jet formed in the initial collapse and bounce (*43*). Therefore, in addition to providing a possible means for achieving high Lorentz factors, strong magnetic fields may also provide a possible mechanism for triggering some GRBs.

Achieving the Observed High Jet Powers in Radio Galaxies and Quasars: The Need for Black Hole Rotation and Thick Disks

In addition to the relativistic jet speeds, another parameter that can be compared to the observations is the total jet power. The predicted jet powers from standard accretion disks around black holes are much too low (*44*). One solution to this problem produces the highest jet powers observed, and it also suggests a fundamental explanation for why AGN separate into various classes (such as radio loud or radio quiet) and why jet production in microquasar jets is correlated with the state of the accretion disk (*45*).

Standard accretion disk models indicate that accretion disks should have a substantial toroidal magnetic field strength (B_ϕ) to explain the inward spiraling of material onto the black hole. However, it is the poloidal field protruding from the disk that drives the jet, not the toroidal field, and $B_{\rm p}$ is expected to be only a fraction $(H/R)^n$ of the toroidal field strength, where H is the half-thickness of the disk and $n \sim 1$ (*44*). Equation 4 then becomes

$$L_{\rm MHD} = B_{\phi 0}^2 H_0^2 R_0^2\, \Omega_0^2/32c \qquad (6)$$

If the disk is thin ($H_0 \ll R_0$), as is the case for the standard models (*46*), then $L_{\rm MHD}$ will be small. For a $10^9\,M_\odot$ black hole accreting at 10% of the maximum rate allowed by radiation pressure (the Eddington accretion rate of $\sim 10^{18}$ g s^{-1} $M/M_\odot$), the largest powers generated from a radius $R_0 \sim 7\,R_{\rm g}$ are 10^{42} to 10^{43} erg s^{-1}, several orders of magnitude weaker than the power of $\sim 3 \times 10^{45}$ erg s^{-1} seen in the most powerful radio sources that are thought to harbor a hole of this mass (*47*).

For some accreting sources, however, particularly those that produce hard x-rays, standard disks are not good models. Instead, a geometrically thick ($H_0 \sim R_0$) and hot ($>10^9$ K) disk or torus gives a better fit to the data. Several types of geometrically thick disk models have been proposed, including advection-dominated accretion flows (ADAFs), which carry most of the disk's thermal energy into the black hole (*48*); convection-dominated accretion flows, which include convection as well (*49*); and advection-dominated inflow/outflow solutions, which carry some of the disk's internal energy outward in a thermal wind (*50*). Because the poloidal magnetic field strength [$B_{\rm p} \sim (H_0/R_0)\,B_\phi$] increases with disk thickness, the vertical magnetic field should be much stronger in thick disks than in thin ones, leading to much stronger jets. However, when the ADAF solutions, for example, are used to evaluate Eq. 6, the results yield a jet power not much above 10^{44} erg s^{-1} (still a factor of 30 below the most luminous observed jets). The jet power is low because, although thick disks have strong fields, they are partially pressure supported and so do not rotate at the Keplerian rate.

One way to generate the highest observed radio jet powers is to place the thick accretion disk around a rapidly rotating Kerr black hole. The frame dragging near the hole's ergosphere produces a differential rotation that is nearly as rapid as Keplerian rotation, making both H_0 and Ω_0 large in Eq. 6. With $R_0 \sim 2\,R_{\rm g}$ as the characteristic radius of the jet-production region near a Kerr hole and a mass accretion rate of 10% of the Eddington limit, the predicted jet power for a rapidly rotating $10^9\,M_\odot$ black hole is a few times 10^{45} erg s^{-1}, similar to the maximum observed. The idea that rapidly rotating black holes produce strong radio jets and slowly rotating holes produce weak sources is called the spin paradigm. It provides a possible explanation for why radio loud and radio quiet quasars look so similar in the optical but only some, those with rapidly rotating black holes, have radio jets (*51*).

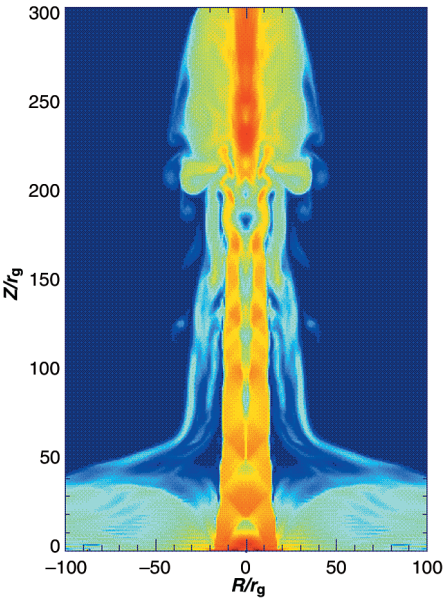

Fig. 8. Illustration of an efficient high MHD power jet, with $L_{\rm MHD} = 1.5L_{\rm crit}$ [from (*54*)]. The diagram shows the strength of the magnetic pressure ($B^2/8\pi$) at a model time of ~10 inner disk rotation times, with red indicating the strongest pressure and blue indicating the weakest. Acceleration occurs much faster than the dynamical rate. The flow reaches a quasi–steady state quickly, with a tightly collimated jet above the escape speed. Although more powerful, the jet delivers its thrust in a narrow solid angle, affecting the surrounding ambient material much less than the slower, broad outflow in Fig. 7.

The Association of Jet Production with Accretion Disk State: Toward Grand Unification of All Accreting Black Holes

The above analysis also predicts that microquasars with black hole engines will contain rotating Kerr black holes, not Schwarzschild black holes, and that jets will be produced only when the accretion disk is geometrically thick and hot. There is strong observational evidence for the second prediction (*52*). In GX 339-4, for example, a jet is produced when the x-ray source is in the low/hard state. In this state, the disk electron temperature is $T \sim 10^9$ K, indicating a thick disk. On the other hand, when the source enters the high/soft state (with a thin $T \sim 10^7$ K disk), the jet radio emission disappears to a level at least 35 times weaker than that in the low/hard state. Equation 6 predicts a suppression factor of ~100 between geometrically thin and thick disks around a Kerr black hole, consistent with the observed value (*45*).

Little is known about the relation between jet production in the more massive accreting black holes (such as Seyfert galaxies, radio galaxies, and quasars) and the state of their constituent accretion disks. However, a similar association of hot thick accretion flow with the strongest jets is expected. Accretion states similar to those in binary black holes also should exist in supermassive black holes. Different types of hard and soft Seyfert galaxies may be an example of this (*53*). In those sources that display jets, the jet should be produced only when the disk is in a hard accretion state (either a steady low/hard state or an unstable very high state that cycles through both soft and hard periods) and not when the disk emission is soft. Testing this prediction in quasars will require statistical studies, because the typical limit cycle time is expected to be hundreds to thousands of years. Confirmation of this effect will provide additional evidence for a grand unification of all accreting black hole sources, stellar and supermassive alike, and for the MHD production model of relativistic jets.

References and Notes

1. R. C. Vermeulen, *IAU Symp.* **175**, 57 (1996).
2. J. A. Biretta, W. B. Sparks, F. Macchetto, *Astrophys. J.* **520**, 621 (1999).
3. F. Macchetto *et al.*, *Astrophys. J.* **489**, 579 (1997).
4. I. F. Mirabel, L. F. Rodriguez, *Annu. Rev. Astron. Astrophys.* **37**, 409 (1999).
5. B. Margon, *Annu. Rev. Astron. Astrophys.* **22**, 507 (1984).
6. L. Wang *et al.*, *Astrophys. J.* **467**, 435 (1996).
7. A. M. Khokhlov *et al.*, *Astrophys. J.* **524**, L107 (1999).
8. R. A. M. J. Wijers *et al.*, *Mon. Not. R. Astron. Soc.* **294**, L13 (1998).
9. M. Nakamura *et al.*, *New Astron.*, in press.
10. C. F. Michel, *Astrophys. J.* **158**, 727 (1969).
11. P. Goldreich, W. H. Julian, *Astrophys. J.* **160**, 971 (1970).
12. S. D'Odorico *et al.*, *Nature* **353**, 329 (1991).
13. Images are available at http://chandra.harvard.edu/photo/0052/ and http://chandra.harvard.edu/photo/cycle1/vela/.
14. J. M. LeBlanc, J. R. Wilson, *Astrophys. J.* **161**, 541 (1970).
15. G. S. Bisnovatyi-Kogan, *Sov. Astron. A.J.* **14**, 652 (1971).
16. D. L. Meier *et al.*, *Astrophys. J.* **204**, 869 (1976).
17. R. Lovelace, *Nature* **262**, 649 (1976).
18. R. D. Blandford, *Mon. Not. R. Astron. Soc.* **176**, 465 (1976).
19. _____, R. Znajek, *Mon. Not. R. Astron. Soc.* **179**, 433 (1977).
20. R. D. Blandford, D. Payne, *Mon. Not. R. Astron. Soc.* **199**, 883 (1982).
21. Z.-Y. Li, T. Chiueh, M. C. Begelman, *Astrophys. J.* **394**, 459 (1992).
22. Y. Uchida, K. Shibata, *Publ. Astron. Soc. Jpn.* **37**, 515 (1985).
23. K. Shibata, Y. Uchida, *Publ. Astron. Soc. Jpn.* **38**, 631 (1986).
24. R. Matsumoto *et al.*, *Astrophys. J.* **461**, 115 (1997).
25. Y. Uchida *et al.*, *Astrophys. Space Sci.* **264**, 195 (1999).
26. Y. Uchida *et al.*, *IAU Symp.* **195**, 213 (2000).
27. T. Kudoh, R. Matsumoto, K. Shibata, *Astrophys. J.* **508**, 186 (1998).
28. S. Koide, K. Shibata, T. Kudoh, *Astrophys. J.* **495**, L63 (1998).
29. _____, *Astrophys. J.* **522**, 727 (1999).
30. S. Koide *et al.*, in *Proceedings of the 19th Texas Symposium on Relativistic Astrophysics*, E. Aubourg, T. Montmerle, J. Paul, Eds. (World Scientific, Paris, 1999), 01/15, pp. 1–10.
31. S. Koide *et al.*, *Astrophys. J.* **536**, 663 (2000).
32. G. V. Ustyugova *et al.*, *Astrophys. J.* **439**, L39 (1995).
33. R. Ouyed, R. E. Pudritz, *Astrophys. J.* **482**, 712 (1997).
34. R. Krasnopolsky, Z.-Y. Li, R. D. Blandford, *Astrophys. J.* **526**, 631 (1999).
35. I. F. Mirabel *et al.*, *Astron. Astrophys.* **330**, L9 (1998).
36. V. Dhawan, I. F. Mirabel, L. F. Rodriguez, *Astrophys. J.* **543**, 373 (2000).
37. W. Junor, J. A. Biretta, M. Livio, *Nature* **401**, 891 (1999).
38. J. C. Wheeler, D. L. Meier, J. R. Wilson, in preparation.
39. D. L. Meier *et al.*, *Nature* **388**, 350 (1997).
40. M. Nakamura *et al.*, in *Numerical Astrophysics*, S. M. Miyama *et al.*, Eds. (Kluwer, Dordrecht, Netherlands, 1999), pp. 239–240
41. S. A. Colgate, H. Li, *IAU Symp.* **195**, 255 (2000).
42. G. V. Ustyugova *et al.*, *Astrophys. J.* **541**, L21 (2000).
43. A. I. MacFadyen, S. E. Woosley, *Astrophys. J.* **524**, 262 (1999).
44. M. Livio, G. I. Ogilvie, J. E. Pringle, *Astrophys. J.* **512**, 100 (1999).
45. D. L. Meier, *Astrophys. J.*, in press.
46. N. I. Shakura, R. A. Sunyaev, *Astron. Astrophys.* **24**, 337 (1973).
47. M. J. Ledlow, F. N. Owen, *Astron. J.* **112**, 9 (1996).
48. R. Narayan, I. Yi, *Astrophys. J.* **444**, 231 (1995).
49. R. Narayan, I. V. Igumenshchev, M. A. Abramowicz, *Astrophys. J.* **539**, 793 (2000).
50. M. C. Begelman, R. D. Blandford, *Mon. Not. R. Astron. Soc.* **303**, L1 (1999).
51. A. S. Wilson, E. J. M. Colbert, *Astrophys. J.* **438**, 62 (1995).
52. R. Fender *et al.*, *Astrophys. J.* **519**, L165 (1999).
53. W. N. Brandt, *IAU Symp.* **195**, 207 (2000).
54. D. L. Meier, S. Koide, in *Astrophysical Phenomena Revealed by Space VLBI, Proceedings of the First VSOP Symposium*, H. Hirobayashi *et al.*, Eds. (ISAS, Sagamihara, Japan, 2000), pp. 31–38.

55. Part of this research was carried out at the Jet Propulsion Laboratory, California Institute of Technology, under contract to NASA.